INFLUENCE OF LOADING RATE ON TRANSVERSE PLY CRACK GROWTH IN AERONAUTICAL CFRP LAMINATES

NGUYEN The Hoang, Denys GAMBY and Marie Christine LAFARIE-FRENOT

Laboratoire de Mécanique et de Physique des Matériaux
ENSMA, 1 Av Clément Ader, BP 40109
86961 FUTUROSCOPE – CHASSENEUIL Cedex – France

ABSTRACT

In this research, we address the evolution of matrix cracking in viscoelastic cross-ply laminates made of long Carbon Fibre Reinforced Polymer (CFRP). Monotonic tensile tests performed on $[0_3,90_3]_s$ laminates at 120°C have shown a significant influence of loading rate on cracking development. Several numerical simulations meant to display the effect of possible factors are proposed in turn. First, linear viscoelastic shear-lag approaches using failure criteria are developed to describe cracking evolution as a function of load level, assuming a constant loading rate. Then, a simplified Schapery 1-D model is used to characterize the nonlinear viscoelastic ply behaviour. The Correspondence Principle is applied to compute the time-dependent cracking development. This work shows that the viscoelastic behaviour of undamaged material cannot explain alone the loading rate effect on cracking. On the other hand, the loading rate dependence of critical strength gives good predicted cracking curves, which means that the important rate effect pertains to the damaged viscoelastic material in the process zone close to crack tips.

1. INTRODUCTION

Weight saving and high lifetime demands in aeronautic applications require using CFRP composite laminates in several aircraft structural parts. During a supersonic flight of Concorde's successor travelling at a speed of Mach 2, the surface temperature will range between 100°C and 130°C, depending on the considered area. Under such an environment with high temperatures and mechanical loads, the composites display several failure modes, such as matrix cracking, fibre breakage and delamination. In order to guarantee the structural integrity, transverse matrix cracking must be assessed and monitored as it often precedes other damage events.

The recent literature contains some experimental and analytical studies of the influence of viscoelastic behaviour on matrix cracking. Time dependent matrix cracking in transverse plies of cross-ply carbon/epoxy laminates was experimentally investigated by K.Ogi and Y.Takao [1] and Raghavan and Meshii [2]. Under quasi static loading, it is observed that the matrix transverse cracking growth rate depends upon the loading rate at a high temperature of 110°C [1], or even at room temperature [2]. To the knowledge of the authors, up to now there are very few analytical (linear or nonlinear) viscoelastic models using the fracture mechanics approach to predict crack density as a function of time and applied stress level. A probabilistic failure model has been proposed in [1] giving a good agreement between experimental results and predictions under monotonic loading. However, it provides little physical understanding, though the cracking behaviour can be phenomenologically described.

The matrix cracking evolution under monotonic loading in viscoelastic cross-ply laminates is addressed in this research. The objectives are to model the crack development and to assess the respective contributions of different potential causes that might explain the effect of loading rate on damage process. First, several failure criteria are used in a 1-D linear viscoelastic shear-lag approach to predict cracking evolution. Next, a 2-D linear viscoelastic damage analysis is developed. Then, a simplified 1-D non linear analysis is proposed. The numerical simulation results obtained from the above approaches are finally compared with experimental data concerning crack density observed during uniaxial tensile tests on $\left[0_3^{\circ},90_3^{\circ}\right]_S$ laminates.

2. EXPERIMENTAL RESULTS

A carbon/epoxy composite laminate of the type IM7/977-2 with $\left[0^{o}_{3},90^{o}_{3}\right]_{S}$ stacking sequence, which has a nominal ply thickness of 0.125 mm, has been studied. The coupons, 140 mm long and 20 mm wide, were designed and provided by CCR-EADS (Corporate Research Centre, France, of the European Aeronautic Defence and Space Company). This material is made up of long carbon fibres possessing a high modulus of elasticity and of a two-phase toughened epoxy resin. The thermo-elastic properties of the unidirectional ply experimentally obtained at 120°C are given in Table 1.

Table 1. Elastic properties and coefficients of thermal expansion (CTE) of the unidirectional ply at 120°C

Property		Value
Longitudinal modulus (GPa)	E_{11}	148
Transverse modulus (GPa)	E_{22}	7.12
In-plane Poisson's ratio	ν_{12}	0.326
In-plane shear modulus (GPa)	G_{12}	3.3
Out-of-plane shear modulus (GPa)	G_{23}	1.94
Longitudinal CTE (10^{-6} °C)	α_1	0.23
Transverse CTE (10^{-6} °C)	α_2	30

Monotonic uniaxial tensile tests were conducted on the cross-ply laminates at a temperature of 120°C to measure transverse matrix crack density as a function of applied load [3]. Three different loading rates, producing three respective crosshead velocities (0.01 mm/min; 1 mm/min and 10 mm/min), were imposed. The experimental results are presented in Fig.1. At this temperature, loading rate has a significant influence on cracking. First, it can be seen that the occurrence of the first cracks is delayed when the loading rate increases. Namely, the higher the stress rate, the higher is the first ply failure stress. It is also observed that the higher the loading rate the greater the tensile strength. Moreover, the crack density increases more rapidly as a function of applied stress level if the loading rate decreases.

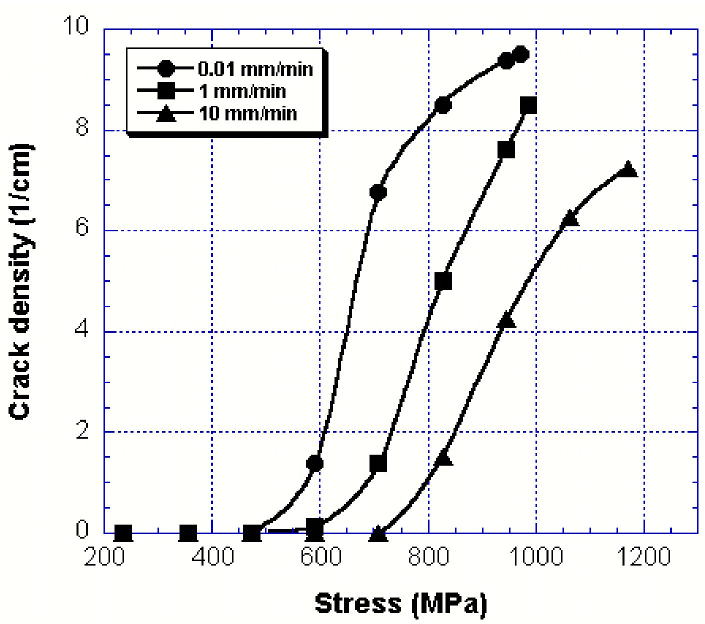

Fig. 1. Effect of loading rate on matrix cracking evolution during monotonic tensile tests at 120°C

3. NUMERICAL SIMULATION OF LOADING RATE EFFECT ON CRACKING

Here, we consider cross-ply composite laminates of the type $\left[0^o_n, 90^o_m\right]_S$ as shown in Fig.2, possessing one 90° layer of thickness $2h_1$ (denoted by superscript (1)) and two outer 0° layers of thickness h_2 (denoted by superscript (2)). The x, y, z directions are the loading direction, the width direction and the thickness direction, respectively. The laminate is subjected to a monotonic tensile loading of form $\overline{\sigma}(t) = \dot{\overline{\sigma}} \times t$, where $\overline{\sigma}$ is the external applied stress in the x direction, $\dot{\overline{\sigma}}$ is the constant loading rate and t denotes the time.

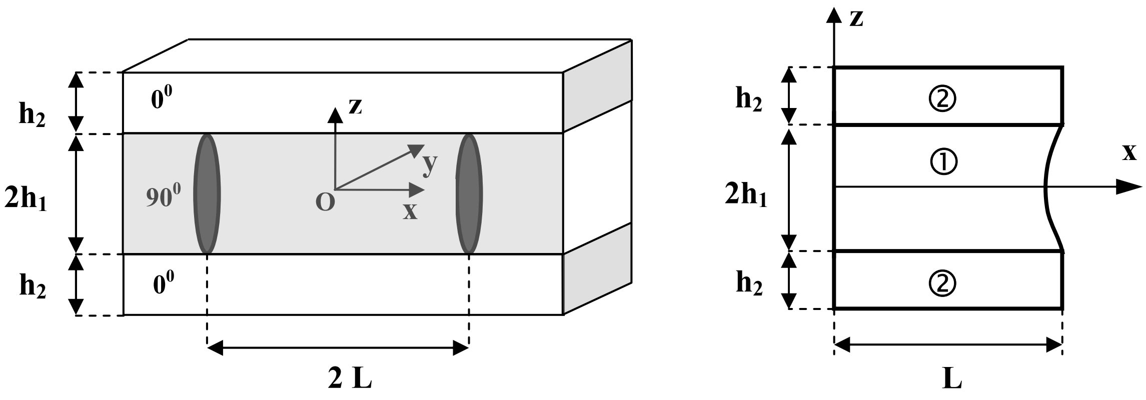

Fig. 2. Laminate and crack geometries

3.1. One dimensional linear analysis

In this section, the one dimensional viscoelastic response of the laminate will be considered. We also take into account residual thermal stresses (at 120°C) in this analysis. First, we find the stress and strain responses of the undamaged laminate in the case when there is no transverse matrix crack. The outer 0° layers and the inner 90° layer are supposed to display elastic and viscoelastic behaviours in the x-direction, respectively. Let $f(t) \otimes g(t) = \int_{0^-}^{t} f(t-\tau) \frac{d}{d\tau} g(\tau) d\tau$ denote the Stieltjes convolution of time functions $f(t)$ and $g(t)$; the constitutive and equilibrium equations of the undamaged laminate can be written in the form:

$$\tilde{\varepsilon}_{x0}(t) - \alpha_1 \Delta T = J_{11}\, \tilde{\sigma}^{(2)}_{x0}(t) \qquad (1)$$

$$\tilde{\varepsilon}_{x0}(t) - \alpha_2 \Delta T = J_{22}(t) \otimes \tilde{\sigma}^{(1)}_{x0}(t) \qquad (2)$$

$$h_{12}\, \tilde{\sigma}^{(1)}_{x0}(t) + \tilde{\sigma}^{(2)}_{x0}(t) = \left(1 + h_{12}\right) \overline{\sigma}(t) \qquad (3)$$

where $J_{11} = 1/E_{11}$ and $h_{12} = h_1/h_2$; a superimposed tilde denotes the through thickness average of a particular variable; $\tilde{\varepsilon}_{x0}(t)$ is the average x-direction laminate strain; $\tilde{\sigma}^{(i)}_{x0}(t)$ is the average stress in layer i (i=1,2); $\Delta T = T_a - T_0$ is the difference between specimen temperature, T_a (120°C), and the stress-free temperature, T_0 (180°C); $J_{22}(t)$ is the creep function of the material such that $E_{22}(t) \otimes J_{22}(t) = H(t)$, H(t) being the Heaviside step function. The equation system can be solved by using the Laplace transform. For this purpose, the tensile compliance in the transverse direction $J_{22}(t)$ is represented in the form: $J_{22}(t) = J_{20} + \sum_{n=1}^{3} J_{2n}\left(1 - e^{-t/\tau_n}\right)$, where J_{20} is a constant and τ_n is the retardation time related to the amplitude J_{2n} . The identification of these material constants obtained from creep/recovery tests on [90°] specimens is presented in Table 2.

Table 2. Parameters of transverse direction compliance at 120°C

Term	Coefficient J_{2n} (Pa^{-1})	Retardation time τ_n (minute)
0	1.335×10^{-10}	
1	2.500×10^{-12}	20
2	1.555×10^{-12}	500
3	8.034×10^{-12}	5000

If the tensile applied stress becomes high enough, the 90° plies can crack. The experimental observations show that the matrix crack distribution in the central 90° layer tends to become periodic when the applied load increases. As a result, the damaged laminate is divided into several unit-cells comprised between two existing adjacent cracks assuming a 2L uniform spacing. Due to the symmetry of the cracked laminate, only a half of the unit-cell is considered (Fig.2). The appropriate boundary conditions are given by $U_1(x=0) = U_2(x=0) = 0$ and $\tilde{\sigma}_x^{(1)}(x=L) = 0$, where U_1 and U_2 are respectively the x-direction displacements of the 90° and 0° layers. Taking into account the viscoelastic behaviour of the central layer in the x-direction and the residual thermal strains, the constitutive equations of the layers and the interface can be written in the form:

$$\tilde{\sigma}_x^{(1)}(x,t) = E_{22}(t) \otimes \left[\tilde{\varepsilon}_x^{(1)}(x,t) - \alpha_2 \Delta T\right] \quad (4)$$

$$\tilde{\sigma}_x^{(2)}(x,t) = E_{11}\left[\tilde{\varepsilon}_x^{(2)}(x,t) - \alpha_1 \Delta T\right] \quad (5)$$

$$\tau^*(x,t) = G(t) \otimes \gamma^*(x,t) \quad (6)$$

where $G(t) = E_{22}(t) / \left[2(1-\nu_{23})\right]$ is the shear relaxation function of the 90° layer and $\gamma^* = \gamma_{xz}(x, z = h_1, t)$ is the shear strain due to the shear stress at the interface $\tau^* = \tau_{xz}(x, z = h_1, t)$. Now, using the equilibrium equations of the layers and of the entire laminate, taking into account the boundary conditions at x=0 and x=L, results in the time evolutions of the maximum average normal stress and the maximum average strain between two adjacent cracks in the following form:

$$\tilde{\sigma}_x^{(1)}(0,t) = \tilde{\sigma}_{x0}^{(1)}(t) \times \left[1 - \frac{1}{\cosh(\alpha_{1D} \times L)}\right] \quad (7)$$

$$\tilde{\varepsilon}_x^{(1)}(0,t) = \tilde{\varepsilon}_{x0}(t) - \left[J_{22}(t) \otimes \tilde{\sigma}_{x0}^{(1)}(t)\right] \times \frac{1}{\cosh(\alpha_{1D} \times L)} \quad (8)$$

where $\alpha_{1D} = \sqrt{\dfrac{3}{h_1^2} \times \dfrac{1}{2(1+\nu_{23})}}$, taking into account the fact that $\dfrac{E_{22}}{E_{11}} = 1$ for the material at hand. Several failure criteria will be used in turn (critical stress, critical strain and Reiner-Weissenberg criterion [4]) to predict the crack multiplication as a function of applied load level, assuming a constant loading rate. The first criterion states that a new crack appears in the matrix of the central lamina when the maximum strain attains some critical value depending on the loading rate, that is, $\varepsilon_x^{(1)}(0,t) = \varepsilon_c + k_\varepsilon \left(\dot{\sigma}/\dot{\sigma}_r\right)^n$, where ε_c, k_ε, n are material constants and $\dot{\sigma}_r$ is a reference stress rate. The second criterion is analogous to the first, but it involves the maximum normal stress between two existing cracks, namely $\sigma_x^{(1)}(0,t) = \sigma_c + k_\sigma \left(\dot{\sigma}/\dot{\sigma}_r\right)^m$, where σ_c, k_σ and m are material constants. The last criterion postulates that a new crack forms if the free energy in the central layer attains a critical value depending on the loading rate. The maximum value of the free energy, attained halfway between two adjacent cracks of spacing 2L, is given by:

$$\varphi(0,t) = \frac{1}{2}\left\{1 - \frac{1}{\cosh(\alpha_{1D} \times L)}\right\}^2 \left\{ J_{20}\left[\varepsilon_{x0}^{(1)}(t)\right]^2 + \sum_{n=1}^{3} \frac{J_{2n}}{\tau_n^2}\left[\int_{0^+}^{t} e^{-\frac{t-u}{\tau_n}} \dot{\varepsilon}_{x0}^{(1)}(u)\,du\right]^2 \right\} \qquad (9)$$

and the corresponding criterion is $\varphi(0,t) = \varphi_c + k_\varphi \left(\dot{\sigma}/\dot{\sigma}_r\right)^p$, where φ_c, k_φ et p are material constants.

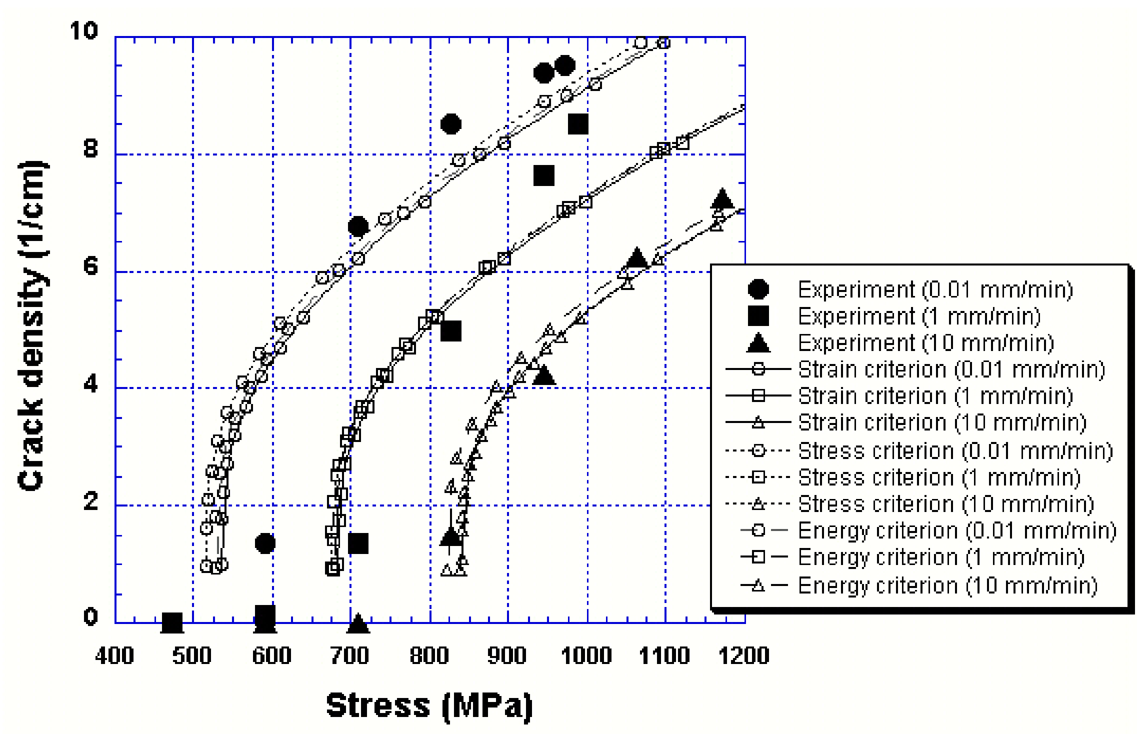

Fig. 3. Measured and predicted cracking evolution at 120°C for three loading rates. Comparison between simulated curves obtained from critical strain criterion (ε_c = 0.0058; k_ε = 0.001; n = 0.23), critical stress criterion (σ_c = 50 MPa; k_σ = 11MPa; m = 0.2), and free energy criterion (φ_c = 0.1975 MNm/m^3; k_φ = 0.065 MNm/m^3; p = 0.25)

Fig.3 presents the resulting numerical simulations of the evolution of the crack density defined by $\rho = \frac{1}{2L}$. The predicted curves are obtained by using the above failure criteria for three values of the loading rate at 120°C. It can be seen that the above criteria give practically the same numerical results and that they allow the experimental data to be well represented only if the critical values depend on the loading rate, which amounts to involve the viscoelastic character of the failing material in the process zone around crack tips.

3.2. Two dimensional linear analysis

The one dimensional analysis does not take into account the viscoelastic character of the outer layers in the y-direction. We now study the impact of this simplification. Using an approach similar to that developed in the unidirectional analysis, we first find the response of the undamaged laminate, then that of the cracked central layer. Using the two dimensional viscoelastic constitutive equations of the layers, and taking into account the laminate symmetry and the boundary conditions, the x-direction maximum stress and strain between two existing adjacent cracks are obtained in the form:

$$\tilde{\sigma}_x^{(1)}(0,t) = \tilde{\sigma}_{x0}^{(1)}(t) \times \left[1 - \frac{1}{\cosh(\alpha_{2D} \times L)}\right] \tag{10}$$

$$\tilde{\varepsilon}_x^{(1)}(0,t) = \tilde{\varepsilon}_{x0}(t) - \left[J_{22}(t) \otimes \tilde{\sigma}_{x0}^{(1)}(t) - \frac{J_{12}^2}{J_{11}} \tilde{\sigma}_{x0}^{(1)}(t)\right] \times \frac{1}{\cosh(\alpha_{2D} \times L)} \tag{11}$$

where $\alpha_{2D} = \sqrt{\frac{3}{h_1^2} \times \frac{1}{2(1+\nu_{23}) + E_{22}/(G_{12}h_{12})}}$; $\tilde{\sigma}_{x0}^{(1)}(t)$ and $\tilde{\varepsilon}_{x0}(t)$ are, respectively, the stress in the 90° layer and the strain of the undamaged laminate subjected to the same loading. They can be found by solving the system of layer constitutive equations, taking into account the "viscoelastic Poisson effect", given in matrix form as [1]:

$$\begin{Bmatrix} \tilde{\varepsilon}_{x0}(t) - \alpha_2 \Delta T \\ \tilde{\varepsilon}_{y0}(t) - \alpha_1 \Delta T \end{Bmatrix} = \begin{bmatrix} J_{22}(t) & J_{12} \\ J_{12} & J_{11} \end{bmatrix} \otimes \begin{Bmatrix} \tilde{\sigma}_{x0}^{(1)}(t) \\ \tilde{\sigma}_{y0}^{(1)}(t) \end{Bmatrix} ; \begin{Bmatrix} \tilde{\varepsilon}_{x0}(t) - \alpha_1 \Delta T \\ \tilde{\varepsilon}_{y0}(t) - \alpha_2 \Delta T \end{Bmatrix} = \begin{bmatrix} J_{11} & J_{12} \\ J_{12} & J_{22}(t) \end{bmatrix} \otimes \begin{Bmatrix} \tilde{\sigma}_{x0}^{(2)}(t) \\ \tilde{\sigma}_{y0}^{(2)}(t) \end{Bmatrix}$$

where $J_{12} = -\nu_{12}/E_{11}$; the stresses in the layers must satisfy the averaged equilibrium equations of the laminate in the x-direction and y-direction, namely $h_{12}\tilde{\sigma}_{x0}^{(1)}(t) + \tilde{\sigma}_{x0}^{(2)}(t) = (1+h_{12})\bar{\sigma}(t)$ and $h_{12}\tilde{\sigma}_{y0}^{(1)}(t) + \tilde{\sigma}_{y0}^{(2)}(t) = 0$. Now the same failure criteria can still be used to predict crack multiplication. Fig. 4 represents the zoomed-in simulation results obtained from a maximum strain failure criterion whose critical value is independent of the loading rate, namely $\tilde{\varepsilon}_x^{(1)}(0,t) = \varepsilon_c$, where ε_c is a constant. In this case, for the three considered loading rates, the numerically predicted crack curves are very close from each other. This proves that, as was the case in the one-dimensional study, a criterion insensitive to the loading rate does not sufficiently convey the influence of the loading rate on cracking, even when taking into account the two-dimensional stress state.

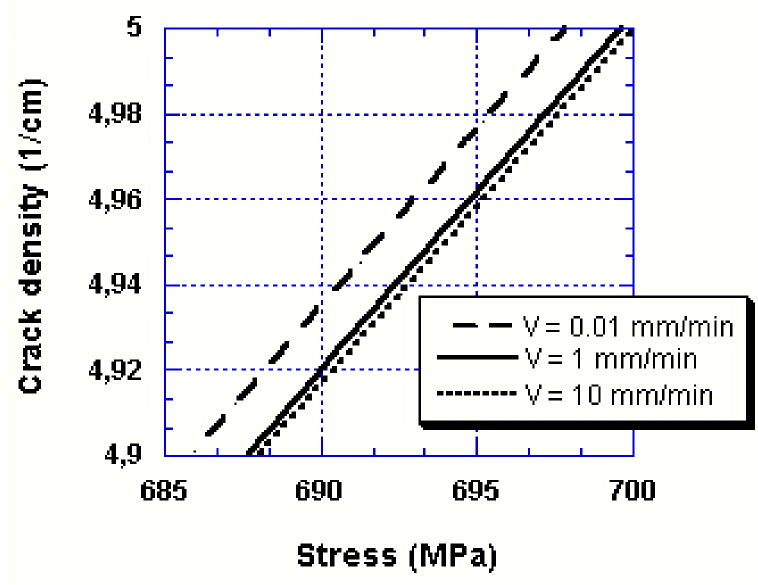

Fig. 4. Predicted cracking evolution at 120°C for three loading rates using a rate-independent critical strain criterion ($\varepsilon_c = 0.0058$)

3.3. One dimensional non linear analysis

The creep tests revealed that the material at hand displays a very marked non linear behaviour, which raises the question whether the non linearity can increase the influence of the loading rate on cracking. A simplified 1-D Schapery model will be used to characterize the non linear viscoelastic behaviour of the 90° layer [5, 6].

Supposing that the non linear behaviour of material in the central layer is described by only one stress-dependent function g_2 [6], we obtain: $\bar{\varepsilon}_x^{(1)}(x,t) = J_{22}(t) \otimes \left\langle g_2(\sigma_{ef})\, \sigma_x^{(1)}(x,z,t) \right\rangle_{2h_1}$, where the symbol $\langle\ \rangle_{2h_1}$ denotes the average of a particular function over the thickness of the central layer, and the effective stress [7] is defined by: $\sigma_{ef}(x,z,t) = \left[\sigma_x^{(1)2} + k_{ef}\, \tau_{xz}^{(1)2}\right]^{1/2}$, with k_{ef} = 3.03 [8]. The nonlinearizing function g_2 can be represented in the form $g_2(\sigma) = 1 + a_g \sigma^{b_g}$, with a_g=0.14 and b_g=2, obtained from creep-recovery tests on [90°] specimens at several stress levels. A possible identification procedure is described in [9]. In order to apply the nonlinear correspondence principle [10], the constitutive equations of the layers must be written in the form:

$$\bar{\varepsilon}_x^{(1)}(x,t) = D(t) \otimes \left\langle J_{20}\, g_2(\sigma_{ef})\, \sigma_x^{(1)}(x,t) \right\rangle_{2h_1} = D(t) \otimes \bar{\varepsilon}_x^{(1)R}(x,t) \tag{12}$$

$$\bar{\varepsilon}_x^{(2)}(x,t) = \frac{1}{E_{11}} \bar{\sigma}_x^{(2)}(x,t) \approx D(t) \otimes J_{11}\, \bar{\sigma}_x^{(2)}(x,t) = D(t) \otimes \bar{\varepsilon}_x^{(2)R}(x,t) \tag{13}$$

where $D(t) = J_{22}(t)/J_{20}$ and the superscript "R" denotes the solution of a reference nonlinear elastic problem corresponding to the nonlinear viscoelastic problem with the same traction boundary conditions. The viscoelastic and elastic stresses are the same, namely $\bar{\sigma}_x^{(i)}(x,t) = \bar{\sigma}_x^{(i)R}(x,t)$ and $\tau^*(x,t) = \tau^{*R}(x,t)$. Taking into account the fact that $\tau^*\, g_2(\sigma_{ef}^*) \approx \tau^*\, g_2\left(\tau^* \sqrt{k_{ef}}\right)$ and $\left\langle \sigma_x^{(1)}\, g_2(\sigma_{ef}) \right\rangle_{2h_1} \approx \bar{\sigma}_x^{(1)}\, g_2\left(\bar{\sigma}_x^{(1)}\right)$ for the material system at hand, the following relationship between stresses can be arrived at:

$$\frac{\partial \tau^{*R}}{\partial x} - \frac{1}{\frac{\partial}{\partial \tau^{*R}}\left[\frac{2h_1}{3}\left(1+\nu_{23}\right)\tau^{*R} g_2\left(\tau^{*R}\sqrt{k_{ef}}\right)\right]}\left\{\frac{J_{11}}{J_{20}}\sigma_x^{(2)R} - \sigma_x^{(1)R} g_2\left(\sigma_x^{(1)R}\right)\right\} = 0 \qquad (14)$$

Combining this with the two following equilibrium equations of the 0° and 90° layers:

$$\frac{\partial \sigma_x^{(1)R}}{\partial x} + \frac{\tau^{*R}}{h_1} = 0 \qquad (15)$$

$$\frac{\partial \sigma_x^{(2)R}}{\partial x} - \frac{\tau^{*R}}{h_2} = 0 \qquad (16)$$

one now obtains a system of nonlinear differential Eqs. (14), (15) and (16), with boundary conditions:

$$\sigma_x^{(1)R}\left(x=L\right)=0 \; ; \; \sigma_x^{(2)R}\left(x=L\right)=\left(1+h_{12}\right)\bar{\sigma}\left(t\right) \; ; \; \tau^{*R}\left(x=0\right)=0 \qquad (17)$$

The unknowns in the above system are the "R" elastic stresses. A numerical program using the shooting method [11] was developed to solve it. Then the maximum viscoelastic strain between two adjacent cracks in the central lamina is found by using Eq. (12). Finally, a critical strain failure criterion is used to model the transverse cracking evolution. A good agreement between the simulated curves and experiments could only be achieved by again introducing the loading rate into the critical values. In Fig. 5, the simulation of crack density curves predicted from 1-D linear and nonlinear analyses, using a rate-dependent critical strain criterion in the central 90° layer, is represented.

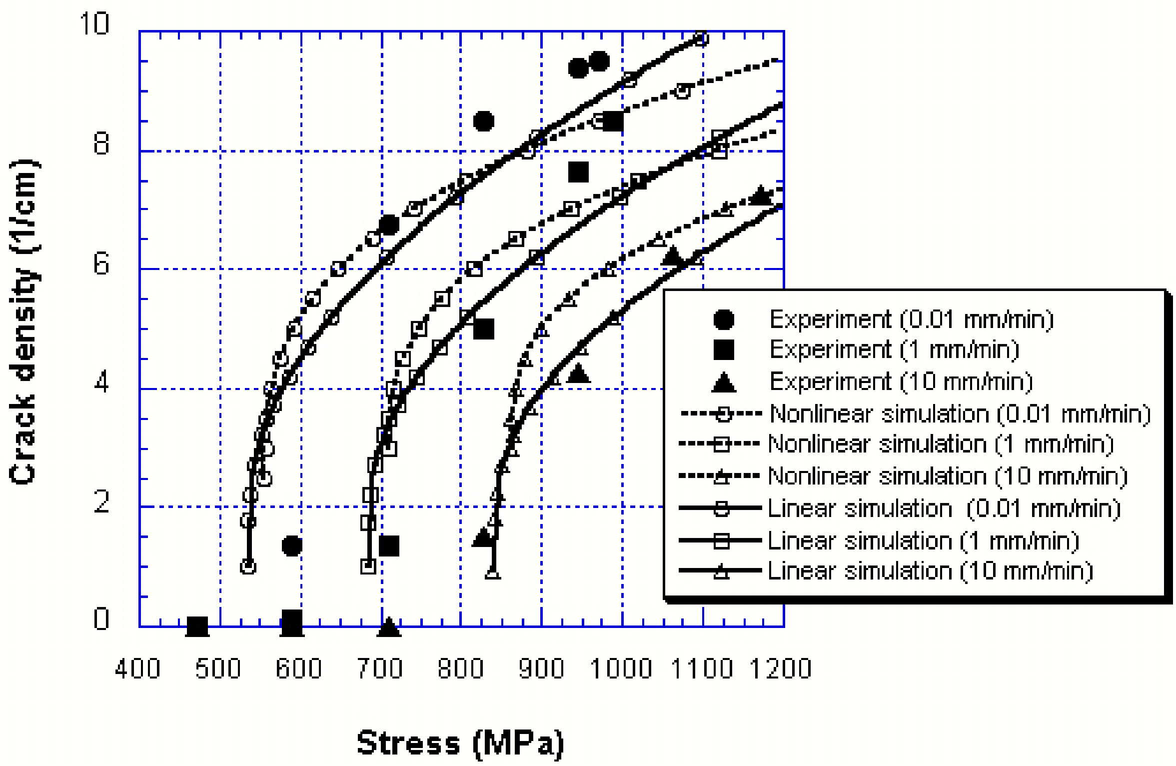

Fig. 5. Crack density (cm^{-1}) versus applied stress (MPa) at 120°C for three loading rates. Comparison between experiment and 1-D linear and nonlinear simulations using a rate-dependent critical strain criterion

4. DISCUSSION AND CONCLUSIONS

The monotonic tensile tests performed on the carbon/epoxy $\left[0^o_3, 90^o_3\right]_S$ at 120°C, with the three respective crosshead velocities (0.01 mm/min, 1 mm/min and 10 mm/min), have displayed a marked loading rate dependence for the transverse matrix cracking evolution. Several phenomena might explain this effect: the viscoelastic behaviour of the undamaged material in the 90° plies and that of the damaged material surrounding the crack tip vicinities.

The aim of this paper is to assess the respective contributions of the different potential causes. For such a purpose, several numerical viscoelastic simulations were proposed in turn.

First, a 1-D linear viscoelastic shear-lag approach, which takes into account thermal stresses, was analyzed. Several failure criteria (critical stress, critical strain and Reiner-Weissenberg free energy density), used to describe cracking evolution as a function of load level assuming a constant loading rate, give very close numerical results. The failure criteria can properly display the loading rate effect only if the stress rate is incorporated.

Next, a 2-D linear viscoelastic analysis was developed. The numerically predicted crack density curves show that, even if the 2-D stress state is taken into account, the viscoelastic character of the undamaged material is not marked enough to explain alone the influence of the loading rate on cracking curves. The improvement brought about by the incorporation of thermal stresses is not significant at the considered temperature.

The simplified 1-D Schapery model was proposed to characterize the nonlinear viscoelastic ply behaviour by using data obtained from creep-recovery tests. A maximum strain failure criterion is used to numerically model the time-dependent cracking evolution. The comparison of 1-D linear and nonlinear numerical results shows that, though important, the material nonlinearity does not significantly enhance the stress rate sensitivity of the damaging process.

This work shows that the viscoelastic behaviour of the undamaged material cannot alone explain the marked effect of the loading rate on transverse cracking. On the other hand, if the loading rate dependence of critical strength is taken into account, good predicted cracking curves are obtained, which means that the observed important rate effect is attributable to the damaged viscoelastic material in the process zone close to crack tips. The precise causes of this loading rate influence remain to be cleared up; cracking tests conducted in a neutral environment will be the next logical step of this research in order to evaluate a possible oxidative effect.

The time-dependent crack density evolution in a viscoelastic laminate subjected to monotonic tensile loading was also modelled. As shown in Fig. 3 and Fig. 5, the predicted cracking curves, for each loading rate, are in good agreement with experiment except for the very early phase of the phenomenon. A probabilistic failure criterion can be attempted in order to better reproduce the S-form of the cracking curves by properly describing the very low crack density range.

References

1. **Ogi, K.** and **Takao, Y.**, "Modeling of time-dependent behaviour of deformation and transverse cracking in cross-ply laminates", *Adv Compos Mater.*, 10 (2001), 39-62.
2. **Raghavan, J.** and **Meshii, M.**, "Time-dependent damage in carbon fibre-reinforced polymer composites", *Compos Part A-Appl S.*, 27 (1996), 1223-1227.
3. **Lafarie-Frenot, M.C., Gamby, D.** and **Nguyen, T.H.**, "Experimental and numerical analysis of loading rate and temperature effects on matrix cracking in CFRP laminates", *P I Mech Eng L-J Mat.*, 218 (2004), 47-53.
4. **Brinson, H.F.**, "Matrix dominated time dependent failure predictions in polymer matrix composites", *Compos Struct.*, 47 (1999), 445-456.

5. **Kennedy, T.C.** and **Wang, M.**, "Three-dimensional, nonlinear viscoelastic analysis of laminated composites", *J Compos Mater.*, 8 (1994), 902–925.
6. **Schapery, R.A.**, "On the characterization of nonlinear viscoelastic materials", *Polym Eng Sci.*, 9 (1969), 295-310.
7. **Schapery, R.A.**, "Nonlinear Viscoelastic and Viscoelastic Constitutive Equations Based on Thermodynamics", *Mech Time-Depend Mat.*, 1 (1997), 209-240.
8. **Allix, O., Ladeveze, P., Le Dantec, E.** and **Vittecoq, E.**, "Damage mechanics for composite laminates under complex loading", *in: Yielding, Damage and Failure of Anisotropic Solids, EGF5 (Edited by J.P. Boehler), Mechanical Engineering Publications, London*, (1990), 551-569.
9. **Gamby D.** and **Blugeon L.**, "On The Characterization by Schapery's Model of Non-linear Viscoelastic Materials", *Polym Test.*, 7 (1987), 137-147.
10. **Schapery, R.A.**, "Correspondence principle and a generalized J integral for large deformation and fracture analysis of viscoelastic media", *Int J Fracture.*, 25 (1984), 195-223.
11. **Press, W.H., Teukolsky, S.A., Vetterling, W.T.** and **Flannery, B.P.**, "Numerical recipes in Fortran", *Second edition, Cambridge University Press, Cambridge*, (1992).